Galectin-7 modulates the length of the primary cilia and wound repair in polarized kidney epithelial cells

Christine Rondanino, Paul A. Poland, Carol L. Kinlough, Hui Li, Youssef Rbaibi, Michael M. Myerburg, Mohammad M. Al-bataineh, Ossama B. Kashlan, Nuria M. Pastor-Soler, Kenneth R. Hallows, Ora A. Weisz, Gerard Apodaca and Rebecca P. Hughey

Am J Physiol Renal Physiol 301:F622-F633, 2011. First published 15 June 2011;
doi: 10.1152/ajprenal.00134.2011

Am J Physiol Renal Physiol 301: F622–F633, 2011.
First published June 15, 2011; doi:10.1152/ajprenal.00134.2011.

Galectin-7 modulates the length of the primary cilia and wound repair in polarized kidney epithelial cells

Christine Rondanino,[1] Paul A. Poland,[1] Carol L. Kinlough,[1] Hui Li,[1] Youssef Rbaibi,[1] Michael M. Myerburg,[2] Mohammad M. Al-bataineh,[1] Ossama B. Kashlan,[1] Nuria M. Pastor-Soler,[1,3] Kenneth R. Hallows,[1,3] Ora A. Weisz,[1,3] Gerard Apodaca,[1,3] and Rebecca P. Hughey[1,3]

[1]*Renal-Electrolyte Division and* [2]*Pulmonary Division, Department of Medicine, and* [3]*Department of Cell Biology and Physiology, University of Pittsburgh School of Medicine, Pittsburgh, Pennsylvania*

Submitted 7 March 2011; accepted in final form 14 June 2011

Rondanino C, Poland PA, Kinlough CL, Li H, Rbaibi Y, Myerburg MM, Al-bataineh MM, Kashlan OB, Pastor-Soler NM, Hallows KR, Weisz OA, Apodaca G, Hughey RP. Galectin-7 modulates the length of the primary cilia and wound repair in polarized kidney epithelial cells. *Am J Physiol Renal Physiol* 301: F622–F633, 2011. First published June 15, 2011; doi:10.1152/ajprenal.00134.2011.—Galectins (Gal) are β-galactoside-binding proteins that function in epithelial development and homeostasis. An overlapping role for Gal-3 and Gal-7 in wound repair was reported in stratified epithelia. Although Gal-7 was thought absent in simple epithelia, it was reported in a proteomic analysis of cilia isolated from cultured human airway, and we recently identified Gal-7 transcripts in Madin-Darby canine kidney (MDCK) cells (Poland PA, Rondanino C, Kinlough CL, Heimburg-Molinaro J, Arthur CM, Stowell SR, Smith DF, Hughey RP. *J Biol Chem* 286: 6780–6790, 2011). We now report that Gal-7 is localized exclusively on the primary cilium of MDCK, LLC-PK_1 (pig kidney), and mpkCCD_{c14} (mouse kidney) cells as well as on cilia in the rat renal proximal tubule. Gal-7 is also present on most cilia of multiciliated cells in human airway epithelia primary cultures. Interestingly, exogenous glutathione *S*-transferase (GST)-Gal-7 bound the MDCK apical plasma membrane as well as the cilium, while the lectin *Ulex europeaus* agglutinin, with glycan preferences similar to Gal-7, bound the basolateral plasma membrane as well as the cilium. In pull-down assays, β1-integrin isolated from either the basolateral or apical/cilia membranes of MDCK cells was similarly bound by GST-Gal-7. Selective localization of Gal-7 to cilia despite the presence of binding sites on all cell surfaces suggests that intracellular Gal-7 is specifically delivered to cilia rather than simply binding to surface glycoconjugates after generalized secretion. Moreover, depletion of Gal-7 using tetracycline-induced short-hairpin RNA in mpkCCD_{c14} cells significantly reduced cilia length and slowed wound healing in a scratch assay. We conclude that Gal-7 is selectively targeted to cilia and plays a key role in surface stabilization of glycoconjugates responsible for integrating cilia function with epithelial repair.

ciliogenesis; polarized epithelia; wound healing

GALECTINS (GAL) ARE A FAMILY of small soluble lectins characterized by the presence of one or two homologous carbohydrate recognition domains with specificity for glycoconjugates that contain β-galactosides (10). To date, 15 mammalian galectins have been identified, each with affinity for a defined subset of carbohydrates (23, 41, 43, 53). Interestingly, galectins are found throughout the cell in the nucleus, cytoplasm, and extracellular compartments where they function in a wide variety of biological processes such as cell adhesion, cell differentiation and development, signal transduction, regulation of cell proliferation and cell death, and membrane trafficking (10, 17, 18).

While nuclear activities of galectins are glycan independent (28), cell surface galectins undoubtedly utilize their carbohydrate recognition domains and multivalency to bind to and crosslink glycoconjugates, as described for Gal-3 interaction with cytokine receptors, Gal-9 interaction with the glucose transporter Glut-2, and Gal-1 interaction with ion channels (24, 37, 39). In each case, the loss of galectin binding correlated with reduced plasma membrane levels of the transmembranous binding partner, indicating that galectins function to stabilize specific proteins at the cell surface (24, 37, 39). Interestingly, galectins do not reach the cell surface through the well-characterized vesicular biosynthetic pathway linking the endoplasmic reticulum and Golgi complex but are released from the cytoplasm in a fully folded form by an "unconventional protein secretion" mechanism (10). Several paths for unconventional secretion of specific proteins have been proposed, including direct transit across the plasma membrane or incorporation into vesicular intermediates such as secretory lysosomes, shed plasma membrane microvesicles, or exosomes (36).

The mechanism of galectin secretion is presently unknown, but both Gal-3 and Gal-4 were observed within distinct transport vesicles released from the *trans*-Golgi network (TGN) of epithelial cells that could represent the pathway for galectin secretion (11, 14, 48, 51). In each case, the galectin was associated with a subset of vesicles carrying cargo with distinct apical-targeting signals. Gal-3 was detected in polarized Madin-Darby canine kidney (MDCK) cells within vesicles carrying the apically targeted neurotrophin receptor (p75), that exhibits a lipid raft-independent targeting signal, at 7.5–10 min after vesicle release from the TGN (13, 15). Depletion of Gal-3 from these kidney cells resulted in missorting of three apical transmembrane glycoproteins including p75, lactase-phlorizin hydrolase (LPH), and gp114 to the basolateral membrane, while trafficking defects of glycoproteins including LPH were observed in the intestines of Gal-3 null mice (13, 16). On the other hand, Gal-4 is associated with vesicles specifically involved in the lipid raft-dependent apical delivery of glycoproteins to the brush-border membrane of polarized enterocyte-like HT-29 cells (14, 51). Recently, Gal-9 was reported to play a role in the sorting and delivery of surface proteins and in the establishment of epithelial polarity in MDCK cells; Gal-9 interaction with the apically enriched Forssman glycosphingolipid was key in this process (32). Altogether, these data are consistent with the hypothesis that galectins exit the cytoplasm

Address for reprint requests and other correspondence: R. P. Hughey, Renal-Electrolyte Div., Dept. of Medicine, Univ. of Pittsburgh School of Medicine, S-933 Scaife Hall, 3550 Terrace St., Pittsburgh, PA 15261 (e-mail: hugheyr@pitt.edu).

by targeted incorporation into vesicles containing specific glycoconjugate-binding partner(s), where they subsequently play a key role in apical targeting.

The presence and function of galectins other than Gal-3, -4, and -9 in vesicular traffic have not been well studied in polarized kidney epithelial cells. Our recent data indicate that transcripts for endogenous galectins in MDCK cells were Gal-3 > Gal-9 > Gal-8 > Gal-1 >>> Gal-4 > Gal-7 (43). We were surprised to find Gal-7 in kidney cells as Gal-7 is considered a marker of all stratified epithelia (including epidermis, cornea, oral cavity, esophagus, and anorectal epithelium), where it contributes to differentiation and development in these tissues (29, 47). Gal-7 is also associated with epithelial cell migration, which plays a crucial role in the reepithelialization process of corneal or epidermal wounds (6, 22). Using in situ hybridization, Gal-7 was reportedly absent in epithelia derived from endoderm (such as intestine, kidney, and lung) despite its identification in a proteomic analysis of cilia isolated from primary cultures of human airway cells (29, 38, 54).

We now report data showing that Gal-7 is localized on the primary cilia of polarized kidney epithelial cells. Additional binding sites are clearly present on both the apical and basolateral plasma membranes, indicating that Gal-7 is specifically targeted to binding partners such as β1-integrin on cilia. Interestingly, we found that knockdown of Gal-7 was associated with shorter cilia and reduced wound repair in polarized cultures of mpkCCD$_{c14}$ cells consistent with a role for Gal-7 in stabilization of key glycoconjugates responsible for integrating cilia function with epithelial repair.

MATERIALS AND METHODS

Reagents and chemicals. All chemicals used were obtained from Sigma (St. Louis, MO) unless otherwise noted.

Antibodies and lectins. Mouse anti-Gal-7 antibodies were from R&D Systems (Minneapolis, MN) and used at a 1:200 for immunofluorescence labeling of cultured cells. Rat anti-zonula occludens (ZO)-1 hybridoma R40.76 culture supernatant (Dr. D. A. Goodenough, Harvard University, Cambridge, MA) was used at a dilution of 1:10. Rabbit antibodies directed against polycystin-1 (PC-1) were a gift from Dr. Oxana Ibraghimov-Beskrovnaya (Genzyme, Framingham, MA). This antibody recognizes the amino-terminal region (LRR domain) of PC-1 (25) and was used at 1:200 dilution. Mouse anti-acetylated tubulin antibodies were from Sigma and used at a 1:100 dilution for staining cells and 1:4,000 dilution for staining tissue (see below). Rabbit anti-β1-integrin antibodies were purchased from Millipore (Ab1952, Temecula, CA) and used at 1:1,500 dilution for immunoblotting. Alexa 488-conjugated goat anti-glutathione *S*-transferase (GST) antibodies were from Invitrogen (Carlsbad, CA) and used at 1:1,000 dilution. All affinity-purified and minimal cross-reacting FITC- and Cy5-conjugated secondary antibodies from Jackson ImmunoResearch Laboratories (West Grove, PA) were used at a 1:200 dilution. Cy3-conjugated secondary antibodies (Jackson ImmunoResearch Laboratories) were used at 1:1,000 dilution.

Mouse and goat antibodies against Gal-3 and Gal-7 were purchased from R&D Systems and used at a 1:1,000 dilution for immunoblotting. Rabbit anti-β1-integrin antibodies are from Millipore and used at 1:1,500 dilution. Horseradish peroxidase (HRP)-conjugated secondary antibodies (Jackson ImmunoResearch Laboratories) were used at 1:10,000 dilution. GST and GST-tagged recombinant canine Gal-7 and Gal-3 were produced and purified as described previously (43). Biotinylated *Ulex europeaus* agglutinin (UEA) was purchased from Sigma, and FITC-conjugated streptavidin was obtained from Invitrogen.

Cell culture. MDCK type II cells and LLC-PK$_1$ cells were cultured in MEM from Cellgro (Herndon, VA) containing 10% (vol/vol) FBS (Hyclone, Logan, UT), and 1% (vol/vol) penicillin/streptomycin at 37°C in a humidified atmosphere containing 5% CO_2. The cells grown on 10-cm dishes were detached with trypsin and EDTA and washed with MEM/FBS. Polarized cells used for microscopy were prepared by adding 10^6 cells to the apical chamber of rat tail collagen-coated, 12-mm diameter Transwells (Costar, Cambridge, MA). Cells were cultured in MEM/FBS for 3–5 days. Where indicated, cells were incubated with 100 mM lactose added to the medium overnight before immunofluorescence labeling.

Human airway epithelial (HAE) cells were prepared from excess pathological tissue following lung transplantation and organ donation under a protocol approved by the University of Pittsburgh Institutional Review Board. Cells were plated on collagen-coated Costar Transwell filters as previously described and used for experiments after 4–6 wk of culture at an air-liquid interface (33).

The mpkCCD$_{c14}$ cells were cultured in growth medium composed of equal volumes of DMEM and Ham's F-12 plus 60 nM sodium selenate, 5 μg/ml transferrin, 2 mM glutamine, 50 nM dexamethasone, 1 nM triiodothyronine, 10 ng/ml epidermal growth factor, 5 μg/ml insulin, 20 mM D-glucose, 2% vol/vol FBS, and 20 mM HEPES, pH 7.4, as described (3). Cells were maintained at 37°C in a humidified 5% CO_2 incubator with medium changes every other day and passaged twice weekly. Cells were subcultured onto Costar Transwell filters 4 days before use in experiments to allow for cell polarization.

Immunofluorescence labeling, confocal microscopy, and image processing. MDCK, LLC-PK$_1$, mpkCCD$_{c14}$, and HAE cells were fixed with 4% (wt/vol) paraformaldehyde (Electron Microscopy Sciences, Hatfield, PA) using the pH-shift protocol as previously described (1, 2). Excess paraformaldehyde was quenched with phosphate-buffered saline containing 20 mM glycine, pH 8.0, and 75 mM NH_4Cl for 10 min at room temperature. Fixed cells were then incubated in block buffer [0.025% (wt/vol) saponin, 8.5 mg/ml of fish skin gelatin in PBS] containing 10% (vol/vol) goat serum for 10 min at room temperature. Cells were incubated with primary antibodies, recombinant GST-galectins, or biotinylated UEA for 1 h at room temperature, washed three times with block buffer for 5 min, and then incubated with fluorescent-labeled secondary antibodies (or FITC-conjugated streptavidin to visualize UEA) for 1 h at room temperature. After three additional 5-min washes with block buffer, the cells were rinsed with PBS, fixed with 4% paraformaldehyde in 100 mM sodium cacodylate buffer, pH 7.4, for 5 min at room temperature, then TOPRO-3 nuclear stain for 5 min where indicated (diluted 1:400, Invitrogen), and then mounted. Where noted, immunolabeling was performed on nonpermeabilized cells.

Imaging was performed on a TCS-SL confocal microscope (Leica, Deerfield, IL) equipped with argon, green helium-neon, and red helium-neon lasers. Images were acquired using a ×100 plan-apochromat oil objective (NA 1.4) and the appropriate filter combination. Settings were as follows: photomultipliers set to 600–800 V, Airy ¼ 1, zoom ¼ 2.0–3.0, Kalman filter (n ¼ 4). Images were collected every 0.25 μm and averaged three times. The images (512 × 512 pixels) were saved in a TIFF format using Volocity software (Improvision, Lexington, MA) and imported in FREEHAND 11.0 (Macromedia, San Francisco, CA).

Confocal microscopy of kidney sections. Experiments were conducted using adult male (350 g) Sprague-Dawley rats (Charles River, Wilmington, MA). All animal experiments followed protocols approved by the University of Pittsburgh Institutional Animal Care and Use Committee. The animals were anesthetized using intraperitoneal pentobarbital sodium injections. The kidneys were fixed via left ventricle perfusion with PBS followed by 4% paraformaldehyde-lysine-periodate (PLP) fixation (31, 40). The kidneys were removed after perfusion, cut into ~0.5-cm sections, and placed in PLP fixative overnight at 4°C. The next day, the tissues were washed three times in

PBS and stored at 4°C in 0.02% sodium azide in PBS. To obtain 4-μm-thick cryostat sections, the PLP-fixed kidney tissue was cryoprotected in 30% sucrose in PBS overnight at 4°C. The tissues were subsequently embedded in OCT Compound (Tissue-Tek, Sakura, Torrance, CA) in a mold and frozen at −30°C. Using a Reichert Frigocut microtome, the sections were picked up on Superfrost Plus microscope slides (Thermo Fisher Scientific, Rockford, IL) as previously described (40, 52).

For immunostaining, cryostat sections on slides were hydrated for 30 min in PBS. The slides were pretreated with 1% SDS, as an antigen retrieval method (5) followed by three 5-min washes in PBS. The slides were preincubated in a blocking solution of 1% BSA in PBS with 0.02% sodium azide for 15 min. The sections were incubated in either primary anti-Gal-7 antiserum raised in mouse (R&D Systems) at 1:100 in Dako diluent (Dako, Carpinteria, CA) for 75 min at room temperature or with anti-acetylated tubulin antibody (Sigma) also raised in mouse (1:4,000). Following the primary antibody incubation, the sections were washed twice for 5 min in high-salt PBS (2.7% NaCl) to reduce nonspecific immunolabeling, followed by one wash in normal-strength PBS. Sections were then incubated for 1 h with secondary antibody at room temperature (goat anti-mouse IgG coupled to FITC, Jackson Immunologicals) and again washed as described above.

Some sections were double stained with anti-acetylated tubulin and anti-Gal-7 antibodies. Both of these primary antibodies were raised in mouse, and therefore, a signal amplification technique was used to allow staining of sections with the first primary antibody without cross-reactivity with the second secondary antibody, as previously published (40). Briefly, the first affinity-purified antibody, anti-acetylated tubulin, was applied to the slides at a dilution of 1:4,000, a concentration too low to be detectable by conventional application. The dilute anti-acetylated tubulin antibody was detected using a tyramide amplification kit (PerkinElmer NEN, Waltham, MA) according to the manufacturer's instructions, with tyramide-FITC as a fluorescent reagent. The sections were first immunolabeled with the mouse anti-acetylated tubulin antibody and tyramide-FITC and then were incubated conventionally with mouse anti-Gal-7 antibody and a secondary donkey anti-mouse antibody coupled to Cy3 (Jackson Immunologicals), as described above.

The sections were then mounted in Vectashield (Vector Laboratories, Burlingame, CA) and examined using a Leica E800 epifluorescence confocal microscope. The final images were imported into Adobe Photoshop for adjustment of levels and to generate the merged image of two channels.

Immunoblotting of galectins. For detection of endogenous Gal-3 and Gal-7 present in cell homogenates or purified GST-tagged recombinant canine Gal-3 and Gal-7, lysates were resolved by SDS-PAGE on a 15% polyacrylamide gel, proteins were transferred to nitrocellulose membranes, and then blocked with 5% BSA in phosphate-buffered saline. The nitrocellulose membranes were incubated with primary antibodies overnight followed by a 1-h incubation with HRP-conjugated secondary antibodies. The secondary antibodies were detected with chemiluminescence reagent (PerkinElmer NEN).

Comparison of apical and basolateral β1-integrin binding by GST-Gal-7. Polarized MDCK cells growing on 24-mm permeable supports in six-well clusters (Costar, Corning, NY) were biotinylated with membrane-impermeant sulfo-NHS-SS-biotin (Thermo Fisher Scientific Pierce) on the apical (6 filters) or basolateral (2 filters) surface on ice as previously described (30). Cells on each filter were subsequently solubilized in 0.4 ml of detergent buffer [60 mM *n*-octyl β-D-glucopyranoside and 0.1% SDS in HEPES-buffered saline (HBS; 150 mM NaCl, 10 mM HEPES-NaCl, pH 7.4)] for 20 min at room temperature with end-over-end rotation on a wheel at room temperature. Cell extracts were moved to a 1.5-ml conical plastic tube and centrifuged at 14,000 rpm for 7 min in a microcentrifuge at 4°C. Samples were incubated overnight with end-over-end mixing with 50 μl avidin conjugated to Sepharose (Thermo Fisher Scientific Pierce). The biotinylated proteins bound to the avidin-conjugated beads were washed with 1 ml 1% Triton X-100 in HBS and then with 1 ml HBS, and bound protein was eluted into 400 μl of HBS containing 0.1% SDS by heating for 2 min at 90°C. The eluted material was diluted fivefold with HBS containing 1% Triton X-100 (and adjusted to 14 mM β-mercaptoethanol). The six apical or two basolateral samples were combined and then divided in half for incubation with either GST-tagged canine galectin-like HSPC15 (negative control) or canine Gal-7. A fresh aliquot of each GST-galectin was prepared for every experiment by affinity purification (starting material ~1 μg) on lactose-conjugated to agarose (25 μl of a 50% slurry) and removal of lactose after subsequent binding to glutathione-conjugated Sepharose (25 μl of a 50% slurry) as previously described (43). The following day, the beads were washed with TNB buffer (50 mM Tris·HCl, pH 8, 150 mM NaCl, 14 mM β-mercaptoethanol) and proteins were eluted by successive incubations for 15 min each on a rotating wheel at 4°C with HBS containing 0.1 M sucrose in TNB buffer (as a control for nonspecific binding) and then 0.1 M lactose in TNB buffer (for specific binding).The eluents (10 μl) were recovered with a Hamilton syringe after centrifugation (10,000 *g* for 30 s), mixed with 10 μl Bio-Rad sample buffer for SDS-PAGE on a Criterion precast 4–15% gradient gel (Bio-Rad Life Sciences, Hercules, CA), and transferred to nitrocellulose (Millipore) for immunoblotting with rabbit anti-β1-integrin and analysis with Bio-Rad Versadoc and Quantity One software.

Generation of a Gal-7-knockdown stable cell line in mpkCCD$_{c14}$ cells. pSM2 plasmids harboring short-hairpin (sh) RNAmir for Gal-7 were obtained from Open Biosystems (Huntsville, AL). The hairpin nucleotide sequence for Gal-7 knockdown was TGCTGTTGACAGTGAGCGCTGCCAGCAGGTTCCATGTAAATAGTGAAGCCACAGATGTATTTACATGGAACCTGCTGGCATTGCCTACTGCCTCGGA for the target sequence in human Gal-7, GCCAGCAGGTTCCATGTAA. Preliminary experiments indicated that this target sequence was also sufficient for knockdown of mouse Gal-7 in mpkCCD$_{c14}$ cells. The shRNAmir construct was subsequently subcloned from pSM2 to pTRIPZ according to the manufacturer's instructions. The pTRIPZ empty vector and pTRIPZ containing a control nonsilencing sequence (Open Biosystems) have Tet-On TurboRFP and shRNAmir expression and produces tightly regulated induction of shRNAmir expression in the presence of doxycycline (DOX). Recombinant lentiviruses were generated by cotransfection of individual plasmids with a mixture of two second-generation packaging vectors [pCMV-ΔR8.2 (35) and pCMV-VSV-G (57), Addgene, Cambridge, MA] into HEK-293T cells (2.0×10^6 cells/10-cm dish) using Lipofectamine 2000 (20 μg lentiviral vector, 15 μg pCMV, and 10 μg VSV-G with 90 μl Lipofectamine 2000/dish) according to the manufacturer's instructions (Open Biosystems). Viral supernatants were harvested 72 h after transfection and then filtered and concentrated using Amicon Ultra 50 centrifugal filter units (Millipore). mpkCCD$_{c14}$ cells seeded in six-well plates were infected with viral particles at a multiplicity of infection of ~2. The cells were then grown for 2 wk in medium containing puromycin (2 μg/ml) to select stably transduced cells. The cells were then expanded, plated on Transwell filters, and then allowed to grow to high resistance for use in experiments.

Determination of cilia length in mpkCCD$_{c14}$ cells. Lentivirus-transduced mpkCCD$_{c14}$ cells were plated on filters 1 day before addition of DOX for 3 days (or not) to induce expression of shRNA directed against Gal-7 or the nonsilencing control shRNA. Cells were fixed, permeabilized, and processed for indirect immunofluorescence to detect acetylated tubulin, a marker for cilia. Images of random fields were captured using a Leica DM6000 B microscope equipped with a ×100 objective, and the lengths of individual cilia (100–200/filter) were measured using Volocity 5.0 software. Cilia lengths for each condition were sorted in ascending order and plotted as length vs. percentile, and as a histogram sorted in bins of 0.25-μm length vs. the number of cilia in each bin. In aggregate data from two independent experiments, cilia length of cells grown with and without DOX were compared using the Mann-Whitney *U*-test.

In vitro wound-healing assay. Lentivirus-transduced cells were plated on 35-mm plastic dishes for 1 day before addition of DOX for 3 days to half of the dishes to induce expression of shRNA directed against Gal-7 or the nonsilencing control shRNA. In vitro wound healing was assayed in confluent cell monolayers as described previously (9, 50). Briefly, cells were scraped using a sterile 10-μl pipette tip. The wounded monolayers were washed twice to remove nonadherent cells. Wound healing was evaluated using a fluorescence inverted microscope (Nikon Eclipse TE2000-U), and 20 random images of the wound were captured at 0 and 4 h after wounding using a digital camera (Nikon E995). In each image, three random measurements of the wound width were carried out using the Adobe Photoshop CS2 software. The difference between the mean values at 0 and 4 h were calculated for each condition, and these values were normalized to the value determined for control lentivirus-transduced cells in the absence of DOX (set as 1). Three independent assays were performed and data are presented as means and SE. Statistical significance was determined using a paired Student *t*-test.

RESULTS

Gal-7 localizes to the primary cilia of polarized MDCK cells. Using semiquantitative RT-PCR, we previously identified the endogenous galectins expressed in MDCK cells and concluded that transcript levels for the galectins varied greatly: Gal-3 > Gal-9 > Gal-8 > Gal-1 >>> Gal-4 > Gal-7, while transcripts for Gal-2 and -12 were not detected even with nested primers (43). Friedrichs et al. (21) also reported that Gal-3 transcripts were 100 times more abundant than transcripts for Gal-1, -8, and -9, and 100,000 times more abundant than transcripts for Gal-12 in MDCK cells using real-time PCR. Although Gal-7 transcript levels were exceedingly low in MDCK cells, we did observe staining with anti-Gal-7 antibodies in polarized, permeabilized MDCK cells using immunofluorescence microscopy. We consistently noted punctate anti-Gal-7 staining above the nuclei and the tight junction marker ZO-1 in the majority of MDCK cells using confocal microscopy (Fig. 1*A*, *a–f*). *X-Z* reconstruction of merged images showed that anti-Gal-7 staining was present on filamentous structures resembling the primary cilia at the apical pole of the cells (Fig. 1*Ag*). To test this possibility, cells were incubated with antibodies against the MDCK primary cilia-associated protein PC-1 (42). Notably, we found that staining for Gal-7 colocalized perfectly with staining for PC-1 at the apical pole (Fig. 1*B*, *a–e*) indicating that Gal-7 is present on the cilia.

Gal-3 was previously localized on the primary cilia of MDCK cells (8, 27). To be certain that our Gal-7 antibodies did not simply cross-react with Gal-3, antibody specificity was tested on various tissue extracts and on purified recombinant proteins by immunoblotting (Supplemental Fig. S1, A and B; all supplementary material for this article is available online at the journal Web site). Anti-Gal-7 consistently recognized only a 15-kDa species while anti-Gal-3 recognized only a 27-kDa species upon immunoblotting mouse tissues, consistent with the molecular weights reported for mouse prototypical-type Gal-7 and chimeric-type Gal-3, respectively. There was also no cross-reactivity between anti-Gal-7 antibodies and recombinant canine Gal-3 (5 μg) or between anti-Gal-3 antibodies and recombinant canine Gal-7 (5 μg) by immunoblotting. Altogether, these data indicate that Gal-7 as well as Gal-3 are localized on the primary cilia of MDCK cells.

As galectins are characterized by their affinity for glycoconjugates containing β-galactose, we asked whether Gal-7 localization on cilia is glycan dependent. To test this possibility, the medium of MDCK cells was supplemented with 100 mM lactose overnight to release Gal-7 from the cell surface. This treatment with lactose (Galβ1,4Glc) was previously demonstrated to deplete endogenous Gal-3 from cells (39) and block exogenous Gal-7 stimulation of wound healing (6). As shown in Fig. 1*C*, *a–d*, all anti-Gal-7 staining was lost by this pretreatment, indicating that Gal-7 association with the primary cilia was glycan dependent.

Gal-7 binds to glycoconjugates on the surface of primary cilia. As growth of MDCK cells with lactose disrupted anti-Gal-7 staining on MDCK cells, we asked whether Gal-7 binding sites on cilia are extracellular and whether the number of sites is limited. To determine whether the binding sites are all extracellular, we incubated freshly prepared recombinant GST-tagged canine Gal-7 with polarized MDCK cells either before or after permeabilization, and before staining with Alexa 488-conjugated anti-GST antibodies. We observed similar staining of cilia-like structures, as well as apical plasma membrane, with anti-GST antibodies after incubation of cells with GST-Gal-7, both with and without membrane permeabilization (Fig. 2*A*, *a–c*, and *B*, *a–c*), indicating that GST-Gal-7 is binding to glycoconjugates only on the extracellular surface of cilia. No anti-GST staining was observed when recombinant GST was added alone to polarized MDCK cells (Fig. 2*A*, *d–f*).

To determine whether binding sites for Gal-7 are limited, GST-Gal-7 binding and colocalization with the cilia-specific intracellular protein acetylated tubulin (20) were compared before and after endogenous Gal-7 was released by overnight pretreatment of the cells with 100 mM lactose in the culture medium. We observed similar levels of staining and perfect colocalization of GST-Gal-7 and acetylated tubulin regardless of whether endogenous Gal-7 was present, indicating that the ligands for Gal-7 binding are not limiting (Fig. 2*C*, *a–*e, vs. *f–j*). GST-Gal-7 binding to the apical plasma membrane differed from the immunostaining of endogenous Gal-7, which was confined to the primary cilia, indicating that Gal-7 is targeted to the cilia by a novel mechanism rather than binding to the cilia after generalized secretion from the cell. Occasional cells (<1%) with bright cytoplasmic staining for Gal-7 were observed in all cultures.

We previously determined that GST-tagged canine Gal-7 preferentially recognizes blood group H (Fucα1,2Gal-R) on type 2 poly-NAc-lactosamine {PL or [Galβ1,4GlcNAcβ1,3]$_n$} with or without internal fucose on PL (Fucα1,3GlcNAc) (43). As the plant lectin UEA also binds blood group H on type 2 PL (but does not tolerate internal fucose) (12), we incubated permeabilized MDCK cells with biotin-conjugated UEA and then FITC-conjugated streptavidin to determine whether blood group H on PL was specific for cilia in MDCK cells. Both primary cilia and basolateral membranes were labeled in cells incubated with UEA (Fig. 3, *A–D*), whereas no staining was observed in the absence of UEA (Fig. 3, *E–H*). These data could indicate either that cilia-specific glycoconjugates recognized specifically by Gal-7 are more complex than blood group H on type 2 PL as defined by UEA binding and/or that Gal-7 binding to cilia results from specific targeting.

Gal-7 binds β1-integrin isolated from either the apical or basolateral surface of MDCK cells. While β1-integrin is localized primarily on the basolateral surface of MDCK cells where it interacts with proteins in the extracellular matrix,

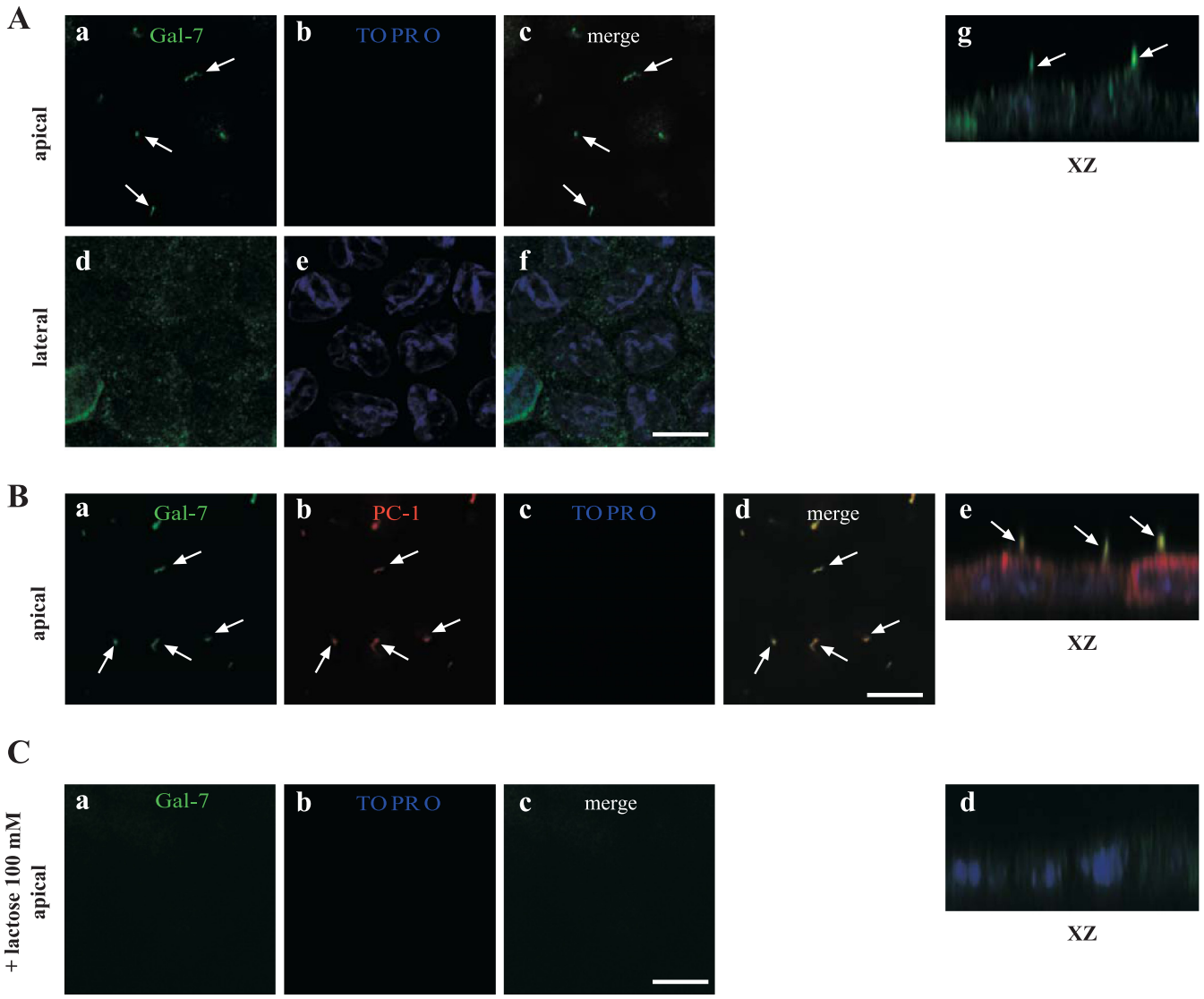

Fig. 1. Galectin-7 (Gal-7) localization in polarized Madin-Darby canine kidney (MDCK) cells. Polarized MDCK cells were fixed, blocked, permeabilized, and incubated with primary antibodies [mouse anti-Gal-7 and rabbit anti-polycystin-1 (PC-1)], then secondary antibodies, before fixation, staining with TOPRO, and mounting for confocal microscopy. *A*: distribution of Gal-7 (green) and the nucleus (blue) at the apical pole (*a–c*) and along the lateral surface (*d–f*) of MDCK cells. Arrows indicate the localization of Gal-7 on the primary cilia. *B*: distribution of Gal-7 (green), PC-1 (a marker of cilia; red), and the nucleus (blue) at the apical pole (*a–d*) of MDCK cells. Arrows indicate colocalization between Gal-7 and PC-1 on the primary cilia. *C*: distribution of Gal-7 (green) and the nucleus (blue) at the apical pole (*a–c*) of MDCK cells grown overnight with 100 mM lactose. Single representative merged images (*Ac*, *Af*, *Bd*, and *Cc*,) and *XZ* sections (*Ag*, *Be*, and *Cd*) are shown. Scale bar = 10 μm.

Praetorius et al. (44, 45) reported that β1-integrin is also present on the primary cilium of polarized MDCK cells. In tumor cells, β1-integrin membrane trafficking and downstream signaling are linked to interactions with Gal-3 and Gal-8 (58), so we tested the possibility that Gal-7 might bind β1-integrin expressed exclusively on the apical (cilia) surface of MDCK cells using a GST-Gal-7 pull-down assay. Polarized cultures of MDCK cells were biotinylated on either the apical or basolateral surface with membrane-impermeant sulfo-NHS-SS-biotin. Cell extracts from six apically biotinylated filters or two basolaterally biotinylated filters were separately combined to obtain a comparable signal for β1-integrin from each cell surface (Fig. 4*A*; see lanes labeled "10% Avidin"). We estimate that only 2% of the surface β1-integrin is on the apical surface. Biotinylated proteins were recovered using avidin-conjugated beads, eluted, and subsequently incubated with either GST-Gal-7 or GST-HSPC15 conjugated to glutathione beads. HSPC15 is an 18-kDa canine galectin-like protein lacking the conserved residues necessary for binding glycoconjugates and thereby acts as a negative control for any nonspecific binding (43).

Using immunoblot analysis of aliquots with anti-β1-integrin antibodies, we found that 100% of the apical-specific β1-integrin and 44% of the basolateral-specific β1-integrin initially bound to the GST-Gal-7-conjugated beads. We did not observe any binding of β1-integrin to the GST-HSPC15-conjugated beads. We observed no elution of β1-integrin when the Gal-7-conjugated beads were subsequently washed with 0.1 M sucrose (a control for nonspecific binding), but we did observe elution of both the apical-specific (92%) and basolat-

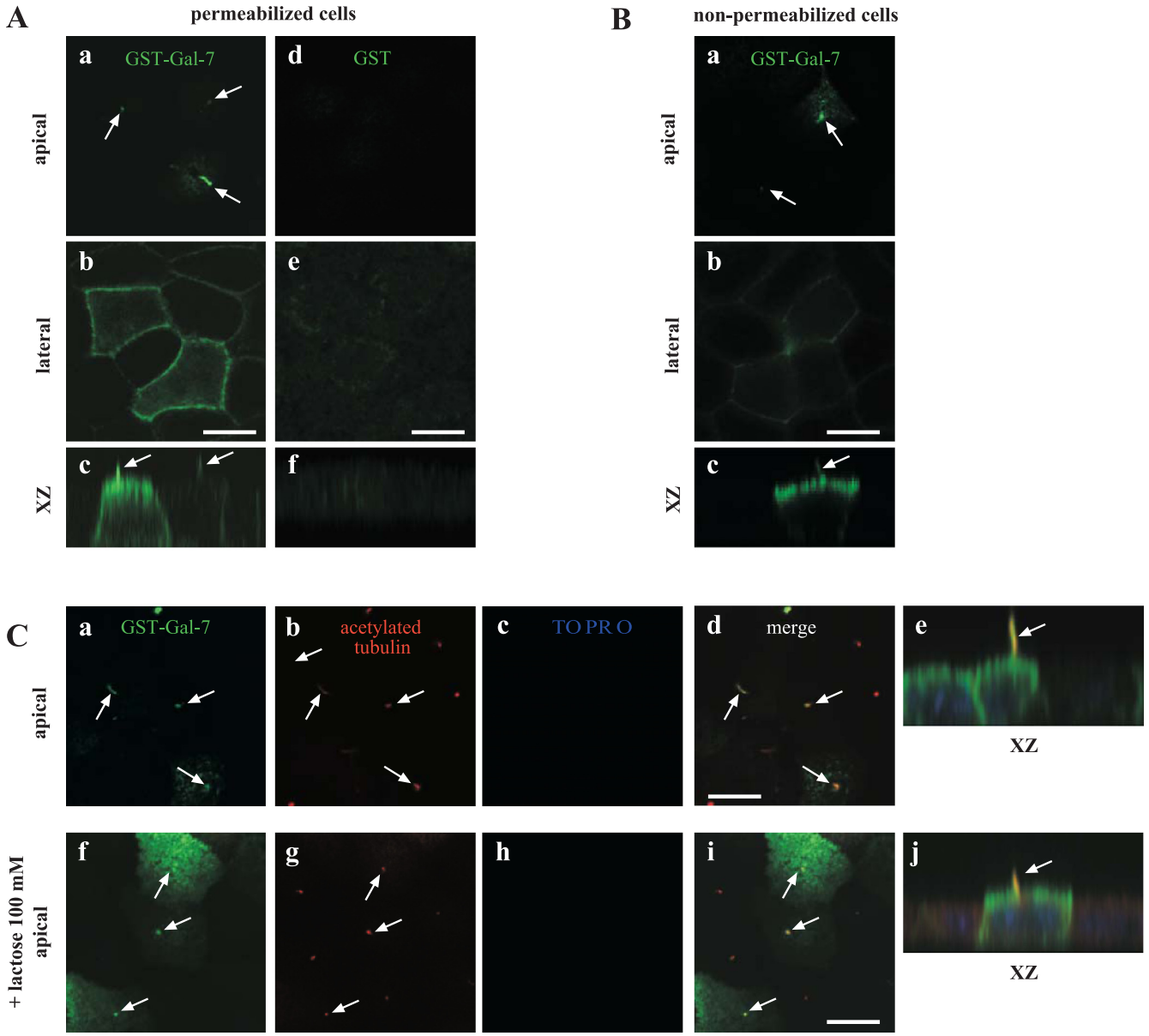

Fig. 2. Recombinant glutathione *S*-transferase (GST)-Gal-7 binding to polarized MDCK cells. Polarized MDCK cells were incubated with recombinant GST-Gal-7 or GST on ice for 1 h before (*B*) or after (*A* and *C*) fixation, permeabilization, and incubation with goat anti-GST (green) or mouse anti-acetylated tubulin (red) primary antibodies. After incubation with secondary antibodies, cells were fixed, stained with TOPRO-3, and mounted for confocal microscopy. Endogenous galectins were released by growing cells overnight in 100 mM lactose before incubation with GST-Gal (*C*, *f–j*). *A*: distribution of GST-Gal-7 or GST at the apical pole (*a* and *d*) and along the lateral surface (*b* and *e*) of MDCK cells. *XZ* sections (*c* and *f*) are shown. Arrows indicate the localization of GST-Gal-7 on the primary cilia. *B*: distribution of GST-Gal-7 at the apical pole (*a*) and along the lateral surface (*b*) of nonpermeabilized MDCK cells. An *XZ* section (*c*) is shown. Arrows indicate the localization of GST-Gal-7 on the primary cilia. *C*: distribution of GST-Gal-7 (green), acetylated tubulin (red), and the nucleus (blue) at the apical pole of MDCK cells (*a–e*) and MDCK cells preincubated with 100 mM lactose (*f–j*). Merged images (*d* and *i*) and *XZ* sections (*e* and *j*) are shown. Arrows indicate colocalization between GST-Gal-7 and acetylated tubulin on the primary cilia. Scale bar = 10 μm.

eral-specific (60%) β1-integrin when the beads were incubated with 0.1 M lactose. Altogether, these data show for the first time that Gal-7 can bind to β1-integrin. As Gal-7 exhibits a similar affinity for binding apically and basolaterally expressed β1-integrin, this indicates that Gal-7 associates exclusively with apically destined β1-integrin (or glycoproteins with similar glycans) targeted to the primary cilium.

Gal-7 is localized on cilia in a variety of cell types. The results of previous studies in human, rat, and mouse tissues using in situ hybridization, Northern blotting, and immunofluorescence microscopy indicated that Gal-7 was expressed in ectodermally derived nonepidermal epithelia such as the esophagus, anorectal region, and buccal cavity but not in epithelia derived from endoderm such as the lining of the intestine, kidney, or lung (29, 54). As we found low but notable expression of Gal-7 in MDCK cells by immunofluorescence microscopy, we looked for Gal-7 expression in kidney cell lines from other species. We observed Gal-7 staining on the primary cilia of both LLC-PK_1 cells (pig) and mpkCCD_{c14} cells (mouse) and GST-Gal-7 binding to cilia of mpkCCD_{c14}

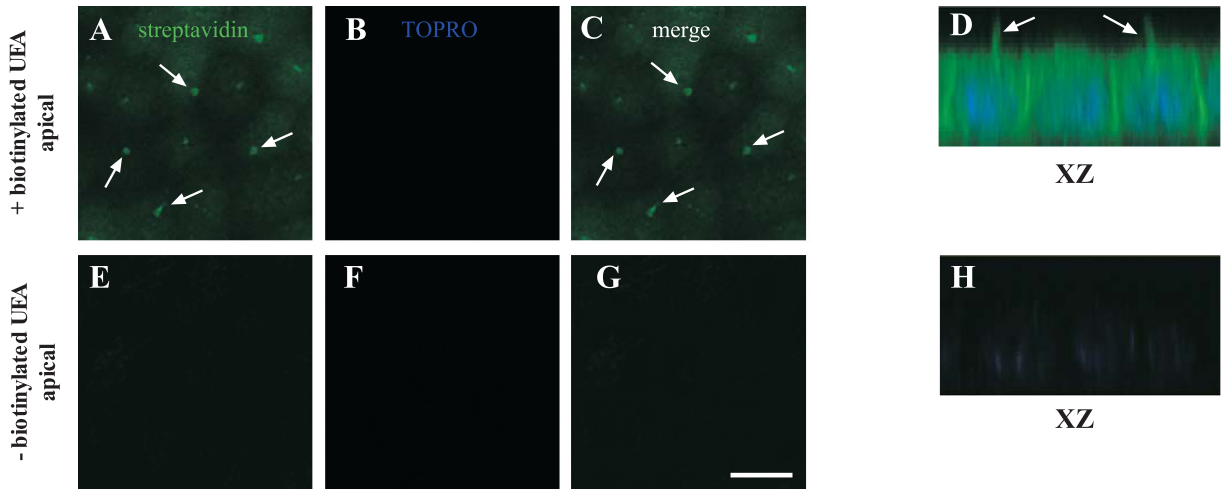

Fig. 3. Localization of H antigen-bearing glycoproteins in polarized MDCK cells. Polarized MDCK cells were fixed, permeabilized, and incubated with or without biotinylated *Ulex europeaus* agglutinin (UEA). Cells were incubated with FITC-conjugated streptavidin (green), fixed, stained with TOPRO-3 (blue), and mounted for confocal microscopy. Representative images are shown for the apical pole of MDCK cells incubated with (*A–D*) or without (*E–H*) UEA are shown. Merged images (*C* and *G*) and *XZ* sections (*D* and *H*) are presented. Arrows indicate the localization of UEA on the primary cilia. Scale bar = 10 μm.

cells (Supplemental Fig. S2). More importantly, we observed costaining for Gal-7 and acetylated tubulin on the primary cilia of the rat renal proximal tubules (Fig. 5*A*, *a–c* and Supplemental Fig. S3) and collecting duct (Pastor-Soler NM, unpublished observations) of rat kidney. We also found colocalization of staining for Gal-7 with PC-1 on many cilia of multiciliated cells in a primary culture of human airway epithelia (Fig. 5*B*, *a–c*) and binding of exogenously added GST-Gal-7, but not GST alone, to cilia from airway (Rondanino C, unpublished observations). Both Gal-3 and Gal-7 were found by immunoblot analysis of extracts from human airway cultures (Supplemental Fig. S4).

Gal-7 knockdown affects cilia length and wound healing in mpkCCD$_{c14}$ cells. The function of Gal-7 has been previously studied only in stratified epithelial cells lacking cilia. To characterize the role of Gal-7 association with the primary cilia of kidney epithelial cells, we knocked down Gal-7 expression using shRNA and assessed the length of cilia. The experiments could not be carried out in MDCK cells because of our inability to effectively measure Gal-7 transcripts with RT-PCR or canine Gal-7 protein levels with immunoblotting and thereby assess knockdown (Rondanino C, Poland PA, and Hughey RP, unpublished observations). In preliminary experiments, we were successful in stable knockdown of Gal-7 expression in primary cultures of human airway cells using lentivirus encoding human-specific shRNA (Li H, Myerburg MM, and Hallows KR, unpublished observations). However, we also found that the same shRNA produced by the lentivirus was efficient in knockdown of mouse Gal-7 in mpkCCD$_{c14}$ cells. As we were successful in immunoblotting mouse Gal-7 in a model of mpkCCD$_{c14}$ cells, we proceeded to study Gal-7 function in the stable kidney cell line rather than the primary airway cultures.

mpkCCD$_{c14}$ cells were stably transduced with a lentiviral vector encoding tetracycline-regulated expression of either an shRNA against Gal-7 or a nonsilencing control shRNA. The lentiviral vector also coexpressed tetracycline-inducible Turbo-RFP. Cells were plated on permeable supports, and the tetracycline analog DOX was added to half of the cultures to induce expression of shRNAs on the following day. After 3 days in culture with or without DOX in the medium, the polarized cells were fixed, permeabilized, and incubated with antibodies against acetylated tubulin to visualize and measure the length

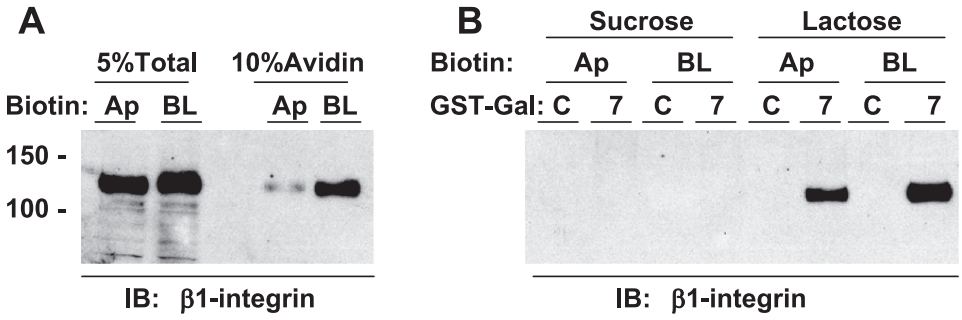

Fig. 4. β1-Integrin from the apical and basolateral surface of polarized MDCK cells binds Gal-7. Polarized MDCK cells were treated with sulfo-NHS-biotin on the apical (6 filters) or basolateral (2 filters) surface, and biotinylated proteins were recovered with avidin-conjugated beads. Proteins recovered from the apical (Ap) or basolateral (BL) surface were pooled and then split in half for incubation with either GST-Gal-7 (7) or galectin-like HSPC15 (control; C) prebound to glutathione-beads. Samples were analyzed by immunoblotting (IB) with rabbit anti-β1-integrin antibodies. *A*: aliquots of total detergent extract (5% total) and recovered biotinylated proteins (10% Avidin) were included as controls. *B*: after overnight incubation, the beads were incubated with sucrose (nonspecific binding), and then lactose (specific binding), and released proteins were recovered for immunoblotting. Numbers on the left indicate the mobility of the Bio-Rad protein standards at 100 and 150 kDa.

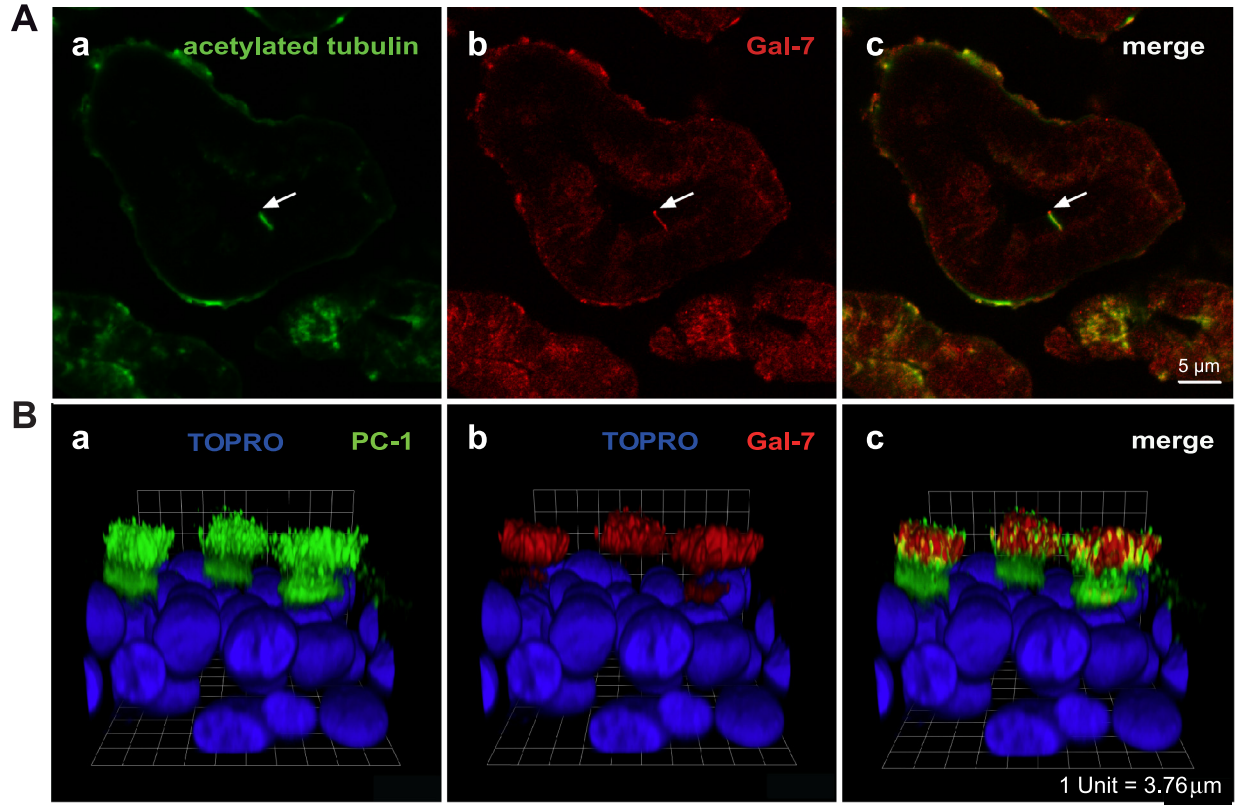

Fig. 5. Gal-7 binds to cilia in rat kidney and cultured human airway cells (HAE). *A*: slices of rat kidney were fixed, embedded, and sectioned before immunostaining with mouse anti-acetylated tubulin (*a*, green) and mouse anti-Gal-7 (*b*, red) antibodies. The merged figure is shown in *c*. Scale bar = 5 μm. Details of the staining protocol for costaining with 2 mouse antibodies are described in MATERIALS AND METHODS. Control images for protocol are presented in Supplemental Fig. S3. *B*: primary cultures of HAE were fixed, permeabilized, and incubated with rabbit anti-PC-1 antibody and mouse anti-Gal-7 antibody. Cells were incubated with secondary antibodies, fixed, stained with TOPRO-3, and mounted for confocal microscopy. 3-Dimensional reconstruction of optical sections taken from the apical to the basolateral surface of the cells shows the distribution of PC-1 (green) and the nucleus (blue; *a*), the distribution of Gal-7 (red) and the nucleus (blue; *b*), and the merged image (*c*). Each segment of the grid is equivalent to 3.76 μm.

of the primary cilia (Fig. 6). Cilia length was measured only in cells expressing TurboRFP (red fluorescent cells) for cultures grown with DOX. Cell extracts were incubated with lactose-conjugated beads and analyzed by immunoblotting with anti-Gal-7 antibodies to assess the level of knockdown (~50%, Fig. 6*B*). We observed significantly shorter cilia in Gal-7-shRNA-expressing cells grown with DOX (knockdown conditions) compared with the same cell line grown without DOX (control conditions), while we observed only a small decrease in the length of the cilia in control shRNA-expressing cells after growth with DOX compared with cells growing without DOX. This is especially evident in Fig. 6*D*, where the peak of cilia of ~1 μm in length is notably increased while the shoulder of cilia between 2 and 4 μm in length is lost when Gal-7 levels are reduced by 50%. Altogether, these data indicate that Gal-7 plays a key role in modulating the length of the primary cilia in mpkCCD$_{c14}$ cells.

As Gal-7 clearly plays a key role in reepithelialization of wounds in the cornea and skin (22, 26), we assessed the role of Gal-7 in wound repair in these same cultures of lentiviral stably transduced mpkCCD$_{c14}$ cells growing on plastic culture dishes with and without DOX in the medium. A sterile pipette tip was used to make a scratch of ~3 μm on each plate. Twenty random microscopic images were obtained of each scratch at 0 h and then at 4 h, a time when the wound was closed halfway (Fig. 7). The data in each of three experiments (n = 60) were normalized such that the rate of wound healing for control shRNA-expressing cells growing without DOX was set as 1. While we observed no difference in the rate of wound healing for control shRNA-expressing cells after growth with or without DOX, we did observe a 33% statistically significant reduction in wound healing for Gal-7-shRNA-expressing cells when grown in DOX. As a similar ex vivo assay for wound healing of keratinocytes from skin explants of Gal-7 knockout mice was reduced by 20% compared with keratinocytes from normal mice (22), we conclude from our studies that Gal-7 plays a significant role in kidney epithelial wound repair.

DISCUSSION

In the present study, we made the novel observation by immunofluorescence microscopy that Gal-7 is localized to the primary cilia of both rat kidney tubules and renal epithelial cell lines from several species (dog, pig, and mouse) as well as the motile cilia of multiciliated lung epithelial cells in primary cultures of human airway tissue. Earlier reports concluded that Gal-7 was primarily expressed in stratified epithelia but was not present in epithelia derived from endoderm such as the lining of the intestine, kidney, or lung (29, 54). Our data indicate that Gal-7 levels are exceedingly low in kidney compared with stratified epithelial cells. However, we observed a robust signal for Gal-7 in immunoblots of cultured human

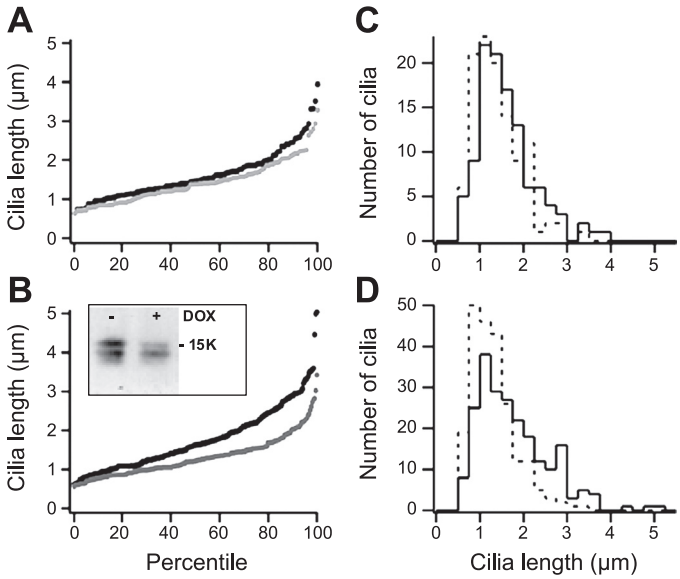

Fig. 6. Cilia length decreases upon knockdown of Gal-7. mpkCCD$_{c14}$ cells stably transduced by lentiviral vectors to express doxycyclin (DOX)-inducible TurboRFP and either control shRNA (*A* and *C*) or short-hairpin (sh) RNA targeting Gal-7 (*B* and *D*) were plated on filter supports for 4 days, with (gray line in *A* and *B*, dashed line in *C* and *D*) or without (black line in *A* and *B*, solid line in *C* and *D*) DOX treatment. Cells were fixed and processed for indirect immunofluorescence using mouse anti-acetylated tubulin antibodies, and cilia lengths of at least 100 cells/condition were quantitated in RFP-positive cells as described in MATERIALS AND METHODS. The cilia lengths were sorted in ascending order for each condition and plotted as either length vs. percentile (*A* and *B*, where each symbol represents a single cilium) or as a histogram with number of cilia (0.25-μm bin size) vs. cilia length (*C* and *D*). In aggregate data from 2 independent experiments, induction of Gal-7 shRNA resulted in a statistically significant decrease in cilia length compared with identical cells plated in the absence of DOX (mean cilia length was 1.30 and 1.77 μm, with and without DOX, respectively, $P < 1 \times 10^{-9}$ by Mann-Whitney *U*-test). Cilia length in cells transduced with control shRNA was slightly different in the presence or absence of DOX (mean cilia length was 1.42 and 1.61 μm, with and without DOX, respectively, $P < 0.03$ using the same analysis).

airway cells (Supplemental Fig. S4), consistent with the identification of Gal-7 in a proteomic analysis of cilia isolated from the same type of cultures (38). Considering the distinct localization of Gal-7 on the cilia of both kidney and lung epithelial cells, and our observations that depletion of Gal-7 in mpkCCD$_{c14}$ cells correlated with shorter cilia length and reduced wound healing, it is likely that Gal-7 has both overlapping and distinct functions in kidney and lung epithelia compared with stratified epithelial cells. As Gal-7 and the primary cilia have been previously linked to epithelial repair (discussed below), Gal-7 most likely functions by stabilizing key glycoconjugates such as β1-integrin on the surface of cilia.

Gal-7 is targeted to the primary cilia in polarized epithelial cells. Cilia are cellular projections formed by a microtubule-based axonemal complex that are assembled on a basal body on the apical surface of polarized epithelia (for a review, see Refs. 19 and 34). These structures can be motile and function in propulsion of fluid, as observed for multiciliated cells of the lung epithelia, or nonmotile, with varied roles in sensing, signaling, and cell proliferation. While small, soluble proteins are delivered into cilia from the cytoplasm by diffusion and retention, structural components of the axoneme are delivered by intraflagellar transport (IFT) using multiprotein complexes and microtubule motors. Interestingly, the cilia membrane lipid and protein content are distinct from that of the plasma membrane. The mechanism for delivery of lipids and transmembrane proteins to cilia most likely involves sorting of these components within the *trans*-Golgi network and budding into specific vesicles destined for the periciliary membrane at the base of the cilia. The targeting of vesicles with cilia-specific cargo is not fully understood and involves targeting sequences, incorporation of specific IFT proteins (IFT20), GTP-Rab8, and rabaptin 5 as well as multiprotein complexes such as the BBsome.

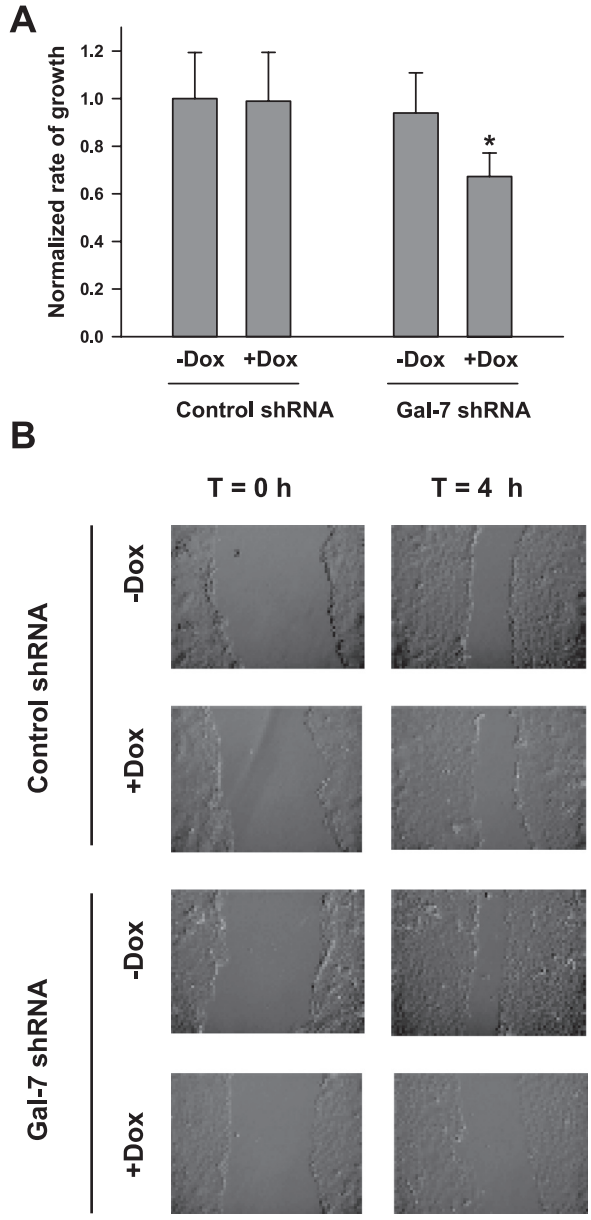

Fig. 7. Wound healing is reduced in cells upon knockdown of Gal-7. mpkCCD$_{c14}$ cells stably transduced by lentiviral vectors to express DOX-inducible TurboRFP and either control shRNA or shRNA targeting Gal-7 were plated on 35-mm dishes for 4 days, with or without DOX treatment, as indicated. Cells were scraped with a sterile pipette tip, and 20 random images of the wound were captured at 0 and 4 h (time for ~50% recovery). Three random measurements of the wound width in each image were carried out using Adobe Photoshop CS2 software. Data from each experiment were normalized to control (−Dox) set as 1, and values of means and SE from 3 experiments are presented here (*$P < 0.01$ by Student's *t*-test; *A*). Representative pictures of the cultures are presented in *B*.

The limited localization of Gal-7 to the primary cilia in the kidney was a surprising observation in light of the patterns we observed for binding of both exogenous GST-Gal-7 and the plant lectin UEA with glycan specificity similar to Gal-7. Exogenous GST-Gal-7 was bound specifically to the apical surface of polarized MDCK cells, including the primary cilia, in the presence or absence of endogenous Gal-7 (−/+ lactose pretreatment), indicating that the number of apical-specific glycoconjugates that can be ligands for Gal-7 are not limiting. Conversely, UEA was bound specifically by the apical cilia and the basolateral membrane, indicating that there are unique glycoconjugates on cilia that are absent from the remainder of the apical surface. Our findings are consistent with the studies by Praetorius et al. (45), who previously identified the normally basolateral β1-integrin as the primary ligand for the cilia-specific binding of the plant lectin *Sambucus nigra* agglutinin (SNA), with preference for sialic acid (NeuAcα2,6Gal or NeuAcα2,6GalNAc). Altogether, it seems that glycoproteins targeted to cilia exhibit a unique array of glycans recognized by SNA, UEA, and Gal-7.

In our present study using surface-specific biotinylation, we found that only 2% of the surface β1-integrin is present on the apical pole of MDCK cells. Small levels of basolaterally targeted/specific proteins are often observed on the apical surface of polarized cells such as MDCK, but the cilia-specific localization of β1-integrin is exceptional and not simply due to mistargeting. While we are not suggesting that β1-integrin is the sole binding partner for Gal-7, it is likely that these two proteins reach the cilia by overlapping pathways. While β1-integrin is a transmembrane glycoprotein requiring a vesicular biosynthetic delivery pathway, Gal-7 is synthesized in the cytoplasm and must cross either the intracellular vesicular membranes or the plasma membrane to reach the luminal or extracellular glycoconjugates of the cilia, respectively, as described for unconventional secretion of other galectins (for a review, see Ref. 36). As we observed that GST-Gal-7 added from the extracellular surface did not exhibit cilia-specific binding but rather bound the entire apical plasma membrane, our cumulative findings are most consistent with Gal-7 transport into biosynthetic vesicles targeted for cilia rather than secretion into the apical compartment. As galectin export from cells is directly linked to the expression of counterligands (i.e., glycan structures) (49), it is quite likely that Gal-7 import into vesicles is directly linked to the presence of Gal-7-preferred glycoconjugates within the vesicle lumen.

Gal-7 plays a key role in wound healing in stratified and simple epithelia. A role for Gal-7 in wound healing has been previously established in keratinocytes and cornea that both lack cilia. Recent studies in Gal-7 null mice that exhibit no obvious skin abnormalities revealed dysregulation of wound healing, with abnormalities in the timing of apoptosis, cell migration, and cell proliferation (22). Cao et al. (6) also found that reepithelialization of corneal wounds was delayed in Gal-3 null mice where secondarily Gal-7 levels were also significantly reduced. Moreover, addition of recombinant Gal-7, but not Gal-3, stimulated wound recovery in corneal explants from Gal-3 null mice, while both Gal-7 and Gal-3 stimulated wound recovery in corneas of normal mice (6). The basis for the reduced expression of Gal-7 in Gal-3 null mice is unknown, and subsequent studies actually found that Gal-7 was actually upregulated in wounded cornea of normal mice (7).

The effectiveness of exogenous Gal-3 and Gal-7 in the studies of corneal wound repair was abrogated by inclusion of lactose, but not sucrose, indicating that the mechanism for stimulating wound repair was glycan dependent (6). Saravanan et al. (46) recently reported that Gal-3 promotes lamellipodia formation in a human corneal epithelial cell line by binding to α3β1-integrin through interactions with the N-linked glycans on the α3-subunit, while Praetorius et al. (44) reported that β1-integrin and α3-integrin are localized on the primary cilium of MDCK cells. We now report that Gal-7 with specificity for linear poly-NAc-lactosamine terminated with blood group H (or sialic acid, NeuAcα2,6) (43) also binds β1-integrin. As Gal-3 is also found on the primary cilium of kidney epithelial cells, where it modulates cilia length (55), and wound healing in lung and kidney epithelial cells has been linked to the transient nature of the primary cilia (4, 56), it seems that Gal-7 and Gal-3 may share binding partners and exhibit some overlapping functions in epithelial homeostasis and repair.

ACKNOWLEDGMENTS

We thank Christy Smolak and Heather Bladek for excellent technical assistance. Dr. A. Vandewalle provided the mpkCCD cells.

GRANTS

This work was supported by the Genzyme Renal Innovations Program (R. P. Hughey) and National Institutes of Health Grants DK54787 (R. P. Hughey), DK054407 (O. A. Weisz), DK075048 (K. R. Hallows), DK084184 (N. M. Pastor-Soler), P30 DK079307 (The Pittsburgh Center for Kidney Research), K08 HL087932 (M. M. Myerburg), and P30 DK072506. C. Rondanino was supported by the Urinary Tract Epithelial Imaging Core of The Pittsburgh Center for Kidney Research.

DISCLOSURES

No conflicts of interest, financial or otherwise, are declared by the authors.

REFERENCES

1. **Apodaca G, Katz LA, Mostov KE.** Receptor-mediated transcytosis of IgA in MDCK cells is via apical recycling endosomes. *J Cell Biol* 125: 67–86, 1994.
2. **Bacallao R, Stelzer EH.** Preservation of biological specimens for observation in a confocal fluorescence microscope and operational principles of confocal fluorescence microscopy. *Methods Cell Biol* 31: 437–452, 1989.
3. **Bens M, Vallet V, Cluzeaud F, Pascual-Letallec L, Kahn A, Rafestin-Oblin ME, Rossier BC, Vandewalle A.** Corticosteroid-dependent sodium transport in a novel immortalized mouse collecting duct principal cell line. *J Am Soc Nephrol* 10: 923–934, 1999.
4. **Blitzer AL, Panagis L, Gusella GL, Danias J, Mlodzik M, Iomini C.** Primary cilia dynamics instruct tissue patterning and repair of corneal endothelium. *Proc Natl Acad Sci USA* 108: 2819–2824, 2011.
5. **Brown D, Lydon J, McLaughlin M, Stuart-Tilley A, Tyszkowski R, Alper S.** Antigen retrieval in cryostat tissue sections and cultured cells by treatment with sodium dodecyl sulfate (SDS). *Histochem Cell Biol* 105: 261–267, 1996.
6. **Cao Z, Said N, Amin S, Wu HK, Bruce A, Garate M, Hsu DK, Kuwabara I, Liu FT, Panjwani N.** Galectins-3 and -7, but not galectin-1, play a role in re-epithelialization of wounds. *J Biol Chem* 277: 42299–42305, 2002.
7. **Cao Z, Said N, Wu HK, Kuwabara I, Liu FT, Panjwani N.** Galectin-7 as a potential mediator of corneal epithelial cell migration. *Arch Ophthalmol* 121: 82–86, 2003.
8. **Chiu MG, Johnson TM, Woolf AS, Dahm-Vicker EM, Long DA, Guay-Woodford L, Hillman KA, Bawumia S, Venner K, Hughes RC, Poirier F, Winyard PJ.** Galectin-3 associates with the primary cilium and modulates cyst growth in congenital polycystic kidney disease. *Am J Pathol* 169: 1925–1938, 2006.
9. **Chung C, Mader CC, Schmitz JC, Atladottir J, Fitchev P, Cornwell ML, Koleske AJ, Crawford SE, Gorelick F.** The vacuolar-ATPase

modulates matrix metalloproteinase isoforms in human pancreatic cancer. *Lab Invest* 91: 732–743, 2011.
10. **Cummings RD, Liu FT.** *Galectins.* Cold Spring Harbor, NY: Cold Spring Harbor Laboratory Press, 2009.
11. **Danielsen EM, van Deurs B.** Galectin-4 and small intestinal brush border enzymes form clusters. *Mol Biol Cell* 8: 2241–2251, 1997.
12. **Debray H, Decout D, Strecker G, Spik G, Montreuil J.** Specificity of twelve lectins towards oligosaccharides and glycopeptides related to N-glycosylproteins. *Eur J Biochem* 117: 41–55, 1981.
13. **Delacour D, Cramm-Behrens CI, Drobecq H, Le Bivic A, Naim HY, Jacob R.** Requirement for galectin-3 in apical protein sorting. *Curr Biol* 16: 408–414, 2006.
14. **Delacour D, Gouyer V, Zanetta JP, Drobecq H, Leteurtre E, Grard G, Moreau-Hannedouche O, Maes E, Pons A, Andre S, Le Bivic A, Gabius HJ, Manninen A, Simons K, Huet G.** Galectin-4 and sulfatides in apical membrane trafficking in enterocyte-like cells. *J Cell Biol* 169: 491–501, 2005.
15. **Delacour D, Greb C, Koch A, Salomonsson E, Leffler H, Le Bivic A, Jacob R.** Apical sorting by galectin-3-dependent glycoprotein clustering. *Traffic* 8: 379–388, 2007.
16. **Delacour D, Koch A, Ackermann W, Eude-Le Parco I, Elsasser HP, Poirier F, Jacob R.** Loss of galectin-3 impairs membrane polarisation of mouse enterocytes in vivo. *J Cell Sci* 121: 458–465, 2008.
17. **Delacour D, Koch A, Jacob R.** The role of galectins in protein trafficking. *Traffic* 10: 1405–1413, 2009.
18. **Elola MT, Wolfenstein-Todel C, Troncoso MF, Vasta GR, Rabinovich GA.** Galectins: matricellular glycan-binding proteins linking cell adhesion, migration, and survival. *Cell Mol Life Sci* 64: 1679–1700, 2007.
19. **Emmer BT, Maric D, Engman DM.** Molecular mechanisms of protein and lipid targeting to ciliary membranes. *J Cell Sci* 123: 529–536, 2010.
20. **Ferrell N, Desai RR, Fleischman AJ, Roy S, Humes HD, Fissell WH.** A microfluidic bioreactor with integrated transepithelial electrical resistance (TEER) measurement electrodes for evaluation of renal epithelial cells. *Biotechnol Bioeng* 107: 707–716, 2010.
21. **Friedrichs J, Torkko JM, Helenius J, Teravainen TP, Fullekrug J, Muller DJ, Simons K, Manninen A.** Contributions of galectin-3 and -9 to epithelial cell adhesion analyzed by single cell force spectroscopy. *J Biol Chem* 282: 29375–29383, 2007.
22. **Gendronneau G, Sidhu SS, Delacour D, Dang T, Calonne C, Houzelstein D, Magnaldo T, Poirier F.** Galectin-7 in the control of epidermal homeostasis after injury. *Mol Biol Cell* 19: 5541–5549, 2008.
23. **Hirabayashi J, Hashidate T, Arata Y, Nishi N, Nakamura T, Hirashima M, Urashima T, Oka T, Futai M, Muller WE, Yagi F, Kasai K.** Oligosaccharide specificity of galectins: a search by frontal affinity chromatography. *Biochim Biophys Acta* 1572: 232–254, 2002.
24. **Huang CL.** Regulation of ion channels by secreted Klotho: mechanisms and implications. *Kidney Int* 77: 855–860, 2010.
25. **Ibraghimov-Beskrovnaya O, Bukanov NO, Donohue LC, Dackowski WR, Klinger KW, Landes GM.** Strong homophilic interactions of the Ig-like domains of polycystin-1, the protein product of an autosomal dominant polycystic kidney disease gene, PKD1. *Hum Mol Genet* 9: 1641–1649, 2000.
26. **Jasti J, Furukawa H, Gonzales EB, Gouaux E.** Structure of acid-sensing ion channel 1 at 1.9 A resolution and low pH. *Nature* 449: 316–323, 2007.
27. **Koch A, Poirier F, Jacob R, Delacour D.** Galectin-3, a novel centrosome-associated protein, required for epithelial morphogenesis. *Mol Biol Cell* 21: 219–231, 2010.
28. **Liu FT, Rabinovich GA.** Galectins as modulators of tumour progression. *Nat Rev Cancer* 5: 29–41, 2005.
29. **Magnaldo T, Fowlis D, Darmon M.** Galectin-7, a marker of all types of stratified epithelia. *Differentiation* 63: 159–168, 1998.
30. **Mattila P, Kinlough CL, Bruns JR, Weisz OA, Hughey RP.** MUC1 traverses apical recycling endosomes along the biosynthetic pathway. *Biol Chem* 390: 551–556, 2009.
31. **McLean IW, Nakane PK.** Periodate-lysine-paraformaldehyde fixative. A new fixation for immunoelectron microscopy. *J Histochem Cytochem* 22: 1077–1083, 1974.
32. **Mishra R, Grzybek M, Niki T, Hirashima M, Simons K.** Galectin-9 trafficking regulates apical-basal polarity in Madin-Darby canine kidney epithelial cells. *Proc Natl Acad Sci USA* 107: 17633–17638, 2010.
33. **Myerburg MM, Harvey PR, Heidrich EM, Pilewski JM, Butterworth MB.** Acute regulation of the epithelial sodium channel in airway epithelia by proteases and trafficking. *Am J Respir Cell Mol Biol* 43: 712–719, 2010.
34. **Nachury MV, Seeley ES, Jin H.** Trafficking to the ciliary membrane: how to get across the periciliary diffusion barrier? *Annu Rev Cell Dev Biol* 26: 59–87, 2010.
35. **Naldini L, Blomer U, Gage FH, Trono D, Verma IM.** Efficient transfer, integration, and sustained long-term expression of the transgene in adult rat brains injected with a lentiviral vector. *Proc Natl Acad Sci USA* 93: 11382–11388, 1996.
36. **Nickel W, Rabouille C.** Mechanisms of regulated unconventional protein secretion. *Nat Rev Mol Cell Biol* 10: 148–155, 2009.
37. **Ohtsubo K, Takamatsu S, Minowa MT, Yoshida A, Takeuchi M, Marth JD.** Dietary and genetic control of glucose transporter 2 glycosylation promotes insulin secretion in suppressing diabetes. *Cell* 123: 1307–1321, 2005.
38. **Ostrowski LE, Blackburn K, Radde KM, Moyer MB, Schlatzer DM, Moseley A, Boucher RC.** A proteomic analysis of human cilia: identification of novel components. *Mol Cell Proteomics* 1: 451–465, 2002.
39. **Partridge EA, Le Roy C, Di Guglielmo GM, Pawling J, Cheung P, Granovsky M, Nabi IR, Wrana JL, Dennis JW.** Regulation of cytokine receptors by Golgi N-glycan processing and endocytosis. *Science* 306: 120–124, 2004.
40. **Pastor-Soler N, Bagnis C, Sabolic I, Tyszkowski R, McKee M, Van Hoek A, Breton S, Brown D.** Aquaporin 9 expression along the male reproductive tract. *Biol Reprod* 65: 384–393, 2001.
41. **Patnaik SK, Potvin B, Carlsson S, Sturm D, Leffler H, Stanley P.** Complex N-glycans are the major ligands for galectin-1, -3, and -8 on Chinese hamster ovary cells. *Glycobiology* 16: 305–317, 2006.
42. **Peters DJ, van de Wal A, Spruit L, Saris JJ, Breuning MH, Bruijn JA, de Heer E.** Cellular localization and tissue distribution of polycystin-1. *J Pathol* 188: 439–446, 1999.
43. **Poland PA, Rondanino C, Kinlough CL, Heimburg-Molinaro J, Arthur CM, Stowell SR, Smith DF, Hughey RP.** Identification and characterization of endogenous galectins expressed in Madin-Darby canine kidney cells. *J Biol Chem* 286: 6780–6790, 2011.
44. **Praetorius HA, Praetorius J, Nielsen S, Frøkiær J, Spring KR.** β1-Integrins in the primary cilium of MDCK cells potentiate fibronectin-induced Ca^{2+} signaling. *Am J Physiol Renal Physiol* 287: F969–F978, 2004.
45. **Praetorius J, Backlund P, Yergey AL, Spring KR.** Specific lectin binding to beta1 integrin and fibronectin on the apical membrane of Madin-Darby canine kidney cells. *J Membr Biol* 184: 273–281, 2001.
46. **Saravanan C, Liu FT, Gipson IK, Panjwani N.** Galectin-3 promotes lamellipodia formation in epithelial cells by interacting with complex N-glycans on alpha3beta1 integrin. *J Cell Sci* 122: 3684–3693, 2009.
47. **Saussez S, Kiss R.** Galectin-7. *Cell Mol Life Sci* 63: 686–697, 2006.
48. **Schneider D, Greb C, Koch A, Straube T, Elli A, Delacour D, Jacob R.** Trafficking of galectin-3 through endosomal organelles of polarized and non-polarized cells. *Eur J Cell Biol* 89: 788–798, 2010.
49. **Seelenmeyer C, Wegehingel S, Tews I, Kunzler M, Aebi M, Nickel W.** Cell surface counter receptors are essential components of the unconventional export machinery of galectin-1. *J Cell Biol* 171: 373–381, 2005.
50. **Sennoune SR, Bakunts K, Martinez GM, Chua-Tuan JL, Kebir Y, Attaya MN, Martinez-Zaguilan R.** Vacuolar H^+-ATPase in human breast cancer cells with distinct metastatic potential: distribution and functional activity. *Am J Physiol Cell Physiol* 286: C1443–C1452, 2004.
51. **Stechly L, Morelle W, Dessein AF, Andre S, Grard G, Trinel D, Dejonghe MJ, Leteurtre E, Drobecq H, Trugnan G, Gabius HJ, Huet G.** Galectin-4-regulated delivery of glycoproteins to the brush border membrane of enterocyte-like cells. *Traffic* 10: 438–450, 2009.
52. **Stevens AL, Breton S, Gustafson CE, Bouley R, Nelson RD, Kohan DE, Brown D.** Aquaporin 2 is a vasopressin-independent, constitutive apical membrane protein in rat vas deferens. *Am J Physiol Cell Physiol* 278: C791–C802, 2000.
53. **Stowell SR, Arthur CM, Mehta P, Slanina KA, Blixt O, Leffler H, Smith DF, Cummings RD.** Galectin-1, -2, and -3 exhibit differential recognition of sialylated glycans and blood group antigens. *J Biol Chem* 283: 10109–10123, 2008.
54. **Timmons PM, Colnot C, Cail I, Poirier F, Magnaldo T.** Expression of galectin-7 during epithelial development coincides with the onset of stratification. *Int J Dev Biol* 43: 229–235, 1999.
55. **Torkko JM, Manninen A, Schuck S, Simons K.** Depletion of apical transport proteins perturbs epithelial cyst formation and ciliogenesis. *J Cell Sci* 121: 1193–1203, 2008.

56. **Weimbs T.** Polycystic kidney disease and renal injury repair: common pathways, fluid flow, and the function of polycystin-1. *Am J Physiol Renal Physiol* 293: F1423–F1432, 2007.
57. **Yee JK, Miyanohara A, LaPorte P, Bouic K, Burns JC, Friedmann T.** A general method for the generation of high-titer, pantropic retroviral vectors: highly efficient infection of primary hepatocytes. *Proc Natl Acad Sci USA* 91: 9564–9568, 1994.
58. **Zick Y, Eisenstein M, Goren RA, Hadari YR, Levy Y, Ronen D.** Role of galectin-8 as a modulator of cell adhesion and cell growth. *Glycoconj J* 19: 517–526, 2004.